20 July 2016

To: Dr. Raymond J. Soukup
Office of Naval Research (Code 322)
875 North Randolph Street
Arlington, VA 22203-1995

From: Dr. Eric I. Thorsos

Subj: ONR Grant N00014-13-1-0216, "Transport Theory for Propagation and Reverberation"

Encl: (1) Final Technical Report
(3) SF298

Enclosure (1) is the Final Technical Report for the subject grant. Enclosure (2) is the SF 298 form which will accompany the final report submission to DTIC. These documents constitute the final deliverables for ONR Grant N00014-13-1-0216.

cc: Grant & Contract Administrator, APL-UW
Office of Sponsor Programs, UW
ONR Seattle – Evan Wood and Kyoohui Beal
Naval Research Laboratory
Defense Technical Information Center

FINAL TECHNICAL REPORT

TRANSPORT THEORY FOR PROPAGATION AND REVERBERATION

by

Eric I. Thorsos
eit@apl.washington.edu, 206-543-1369

Applied Physics Laboratory
University of Washington
1013 NE 40th Street
Seattle, Washington 98105-6698

1. Background and Scope of Effort

There were two main goals proposed for this project on transport theory for propagation and reverberation. The first goal was to make data-model comparisons with TREX13 results for propagation and reverberation to further verify transport theory predictions. A second goal was to use transport theory results to support the development of the TOTLOS model (an effective reflection loss for the total field) that will allow effects of sea surface forward scattering to be incorporated into standard ray-based, mode-based, or energy flux propagation and reverberation models. (Some additional goals were originally proposed, but the reduction in the funds awarded compared to the original amount proposed led to some reduction in goals.)

Propagation or reverberation modeling is typically accomplished using ray tracing, normal mode, or energy flux methods, with PE a common option for propagation. However, these methods usually rely on approximating the effects of forward scattering from roughness at the sea surface or sea floor by using a boundary reflection loss, or by simply ignoring these effects. In order to more accurately treat the full complexity of the environment, full wave methods (which can include mode methods) could be employed, and a "Monte Carlo" approach can in principle be used with realizations of environmental variability, e.g., rough boundaries or water column variability such as internal waves. The average field or average intensity, as well as higher statistics of the field, can then be obtained through averaging results over an ensemble of realizations. The computational burden, however, makes such an approach only suitable for obtaining "benchmark" solutions for comparison with other methods.

The term transport theory applies to any method that attempts to develop evolution equations for the moments (or averages) of the field, and it has been applied to diverse topics quite separate from acoustics. Our approach is based on expanding the acoustic field in modes, and therefore would most readily apply at mid-frequencies and below, and in relatively shallow water environments such as on the continental shelf.

Transport theory, a fast computational method, has been under continuing development in our most recent project, and as implemented it can accurately account for the effects of forward scattering from the sea surface in both propagation and reverberation for frequencies up to the mid-frequency range (e.g., at least up to 3 kHz). We have shown that when applied to reverberation at 3 kHz the effects of surface forward scattering can be quite significant, and without a method such as transport theory that accounts for effects of boundary roughness there can be prediction uncertainties of 10 dB or even greater using traditional modeling methods.

Because of the magnitude of the uncertainty that surface forward scattering introduces into present reverberation modeling, and because transport theory appears to be able to model these effects correctly, it is important to obtain experimental confirmation of transport theory predictions of reverberation. A major focus of the present project has

been to employ reverberation results from TREX13 as a test of transport theory predictions.

The need to account for surface forward scattering with traditional reverberation modeling approaches readily accessable for naval applications is also being addressed. A separate project initially supported by PMW-120 (M. Speckhahn) has been ongoing with this particular goal in mind. The effect of surface forward scattering is treated with an effective surface reflection loss model for the total field (referred to as TOTLOS), where the total field is the combination of the coherent (or reflected) component, and the incoherent (or scattered) component. The original approach in developing TOTLOS was to base it on the results of Monte Carlo rough surface PE results, but as transport theory became available it became clear that results from it were much more suitable to support TOTLOS development. As a result TOTLOS development became an important secondary goal of the present project.

2. Transport Theory Comparisons with PE

Before describing transport theory comparisons with TREX13 results, validations studies of transport theory accuracy using comparisons with parabolic equation (PE) results will be summarized. Past comparisons of propagation field plots between transport theory and PE results have shown excellent agreement. However, that agreement may not be sufficient to validate reverberation predicitions, since the field plots are dominated by the lowest modes, while higher modes excited by surface forward scattering make important contributions to the reverberation level. Thus, a more definitive comparison can be make by comparing the mode amplitudes as a function of range between transport theory and PE. The mode amplitudes are a direct output from transport theory, while more effort is required to obtain the corresponding results with PE. The method used was to make 50 rough surface PE runs with independent realizations of the rough sea surface. For each run the PE field is projected onto modes as a function of range. The absolute square of these mode amplitudes is averaged over realizations and the square root taken to yield rms mode amplitudes as a function of range, which can be compared directly with transport theory mode amplitudes.

Figure 1 shows an example at 3 kHz of the mode amplitude decays obtained from transport theory, where the initial mode amplitudes are all taken equal for convenience of display. Mode coupling occurs from a rough sea surface corresponding to a fully developed sea with a wind speed of 7.7 m/s (15 knots). With a flat sea surface, the mode amplitudes would decrease as straight lines on this plot with a slope that increases monotonically with mode number. The higher mode amplitude density and decrease in slope in the lower part of the plot is due to forward scattering from the surface that leads to mode coupling.

To obtain mode amplitudes with PE, it most convenient to use a point source, which does not yield initial equal amplitudes, and the same point source is used with transport theory. By placing the point source at mid depth (at 25 m depth with a todal depth of 50 m over a sand bottom with attenuation of 0.5 dB/wavelength), the odd numbered modes do begin

with approximately equal amplitudes, while the amplitudes for the even modes are more variable. Thus, plots for odd and even mode numbers are considered separately. Figure 2 gives the comparison for the first 10 odd mode amplitudes showing quite good agreement.
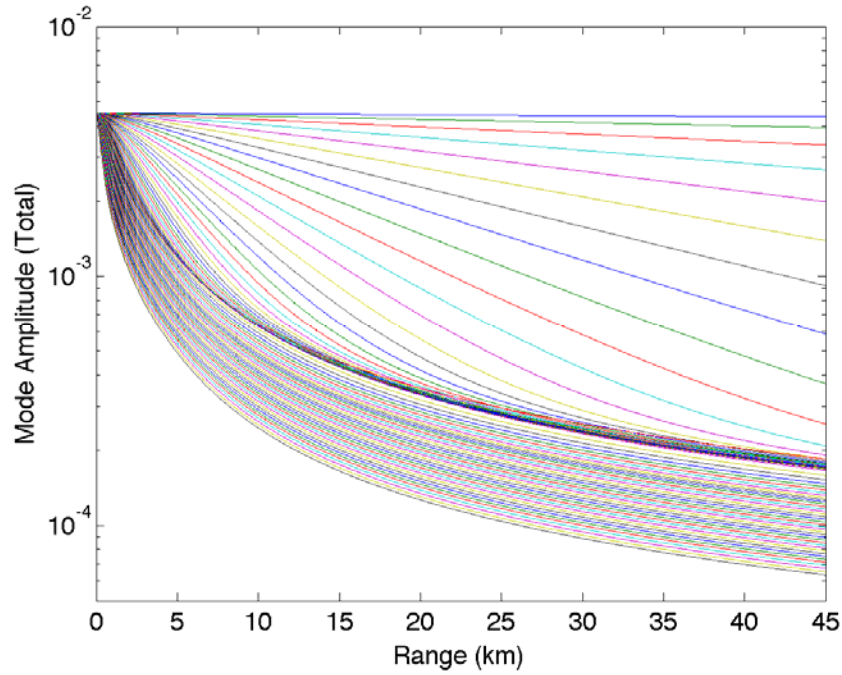

Figure 1. Mode ampitudes for 3 kHz example with initial equal amplitudes. The mode 1 amplitude is the top blue line and the mode numbers increase in order moving down the plot.
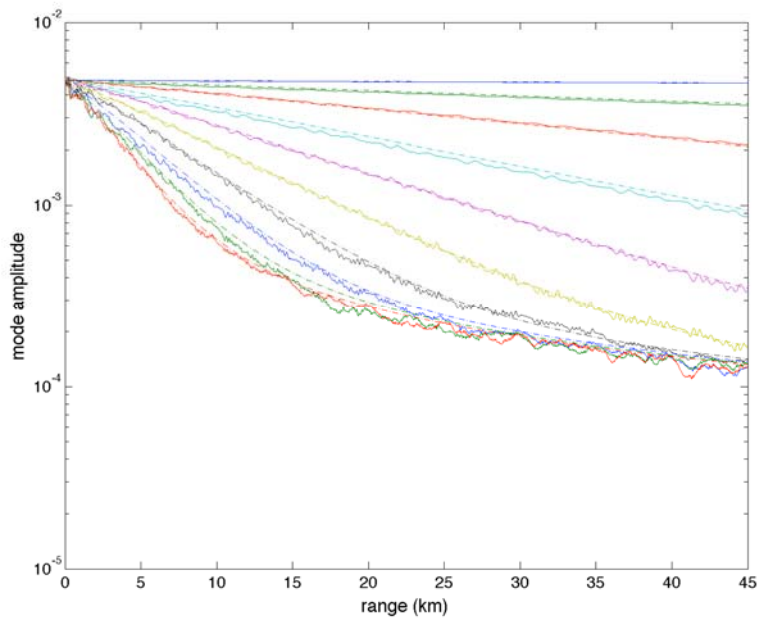
Figure 2. Odd mode decays at 3 kHz comparing transport (smooth dashed lines) and PE (fluctuating lines). Odd mode amplitudes in the range 1–19 are shown.

Figure 3 gives the corresponding comparison for the first 10 even modes, and again the agreement is quite good. However, the comparisons in Figures 2 and 3 are for the lowest modes that corresond to the lowest grazing angles. The algorithm used in our transport theory for mode coupling due to surface roughness is based on first-order perturbation theory, and this method would become the most suspect for higher modes corresponding to higher grazing angles. And these higher modes can make important contributions to reverberation when a rough sea surface leads to mode coupling. Thus it is important as well to verify transport theory accuracy for the highest modes of interest. Figure 4 makes such a comparison, and once again the agreement is quite good. Including even higher modes does not change the reverberation prediction, since convergence with respect to number of modes has been obtained. Thus, the agreement shown in Figure 4 gives strong support to transport theory reverberation predictions up to 3 kHz for a given sea surface roughness spectrum and bottom scattering model. Recall that the PE model does not invoke perturbation theory when treating surface scattering.
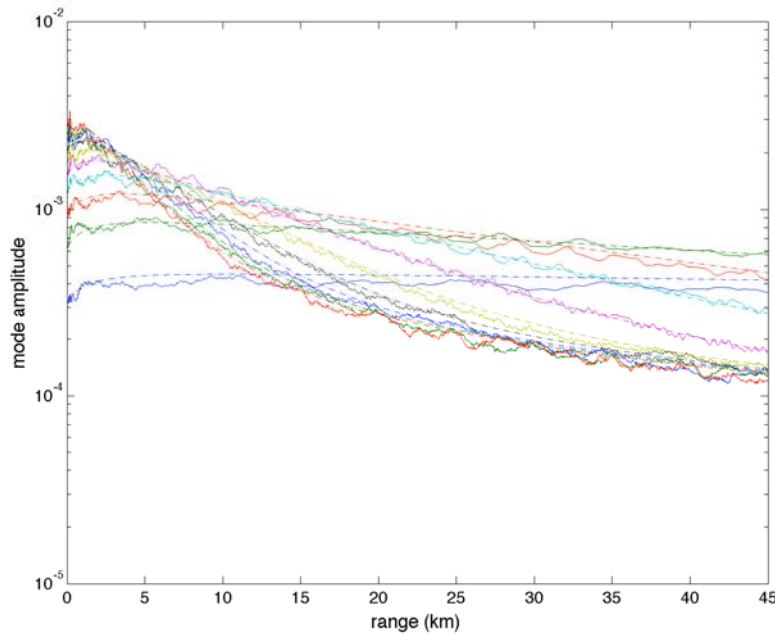

Figure 3. Even mode decays at 3 kHz comparing transport (smooth lines) and PE (fluctuating lines). Even mode amplitudes in the range 2–20 are shown.

3. Data/Model Reverberation Comparisons

TREX13 provided excellent reverberation data sets in a well-characterized environment, and transport theory was used to model the measured reverberation in this shallow water environment at mid frequencies. In doing this, it was necessary to confront the issue of the directional nature of the wave field relative to the "reverberation track," a region of

about 2 degrees in azimuth from which the reverberation was measured with a horizontal array. It must be mentioned that our transport theory method is essentially 2-D (range and depth), so that out-of-plane forward scattering (a 3-D effect) is not treated directly. This fact is important when attempts are made to verify the accuracy of transport theory reverberation predictions by comparisons with measurements. As will be discussed, the reverberation levels can be quite different when the surface waves are closely aligned with the reverberation track compared to when the waves are approximately perpendicular to the reverberation track.
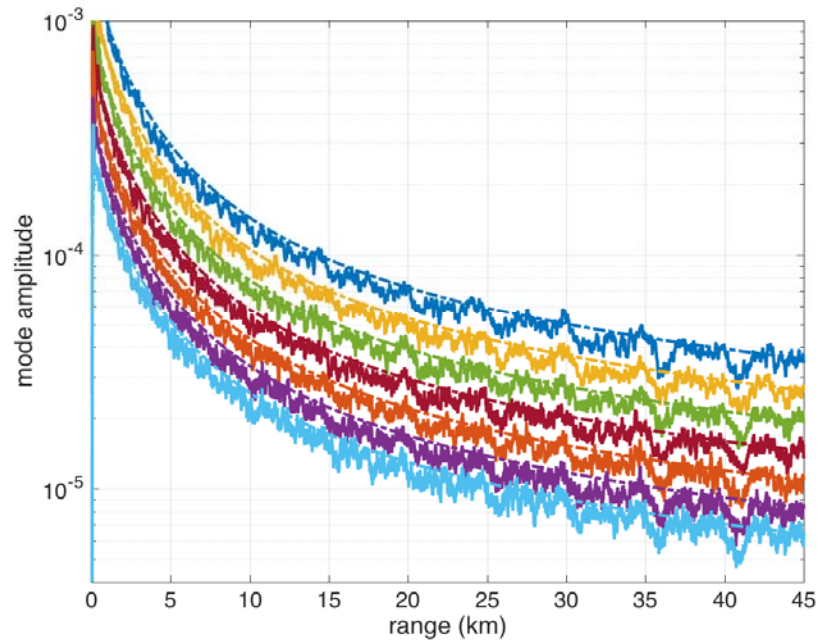

Figure 4. Comparison of mode amplitudes from transport theory (dot-dash lines) and from PE (fluctuating lines) for every tenth mode from mode 80 (top) to mode 140 (bottom). For this case the frequency is 3 kHz, the water depth is 50 m, and there are 70 trapped modes.

To appreciate the complexity that is present when dealing with a 2-D roughness spectrum, it is useful to consider scattering based on perturbation theory in some detail with a plane wave incident on the rough surface. The situation with normal modes will be essentially the same, and perturbation is used to model the coupling of modes. In perturbation theory (also known as Bragg scattering), the horizontal component of an acoustic wave is changed when scattering from a water wave by vector addition and subtraction of the wave vector for the water wave. Let an incident acoustic plane wave have wave vector $\mathbf{k}_i$ = $\mathbf{k}_{iH} + \mathbf{k}_{iz}$, where $\mathbf{k}_{iH}$ denotes the horizontal component and $\mathbf{k}_{iz}$ denotes the vertical component. If the plane wave scatters from a single sinusoidal wave with wave vector $\Delta\mathbf{k}$, which necessarily is in the horizontal plane, then in lowest-order perturbation theory, there are two scattered waves and the horizontal components of the scattered waves are given by $\mathbf{k}_{sH+/-} = \mathbf{k}_{iH} \pm \Delta\mathbf{k}$. The full scattered wave vector for each of these scattered waves is given by $\mathbf{k}_s = \mathbf{k}_{sH} + \mathbf{k}_{sz}$. Because Doppler effects can be ignored in this context,

the magnitudes of the incident and scattered wave vectors can be taken as the same, $|\mathbf{k}_i| = |\mathbf{k}_s|$, which is sufficient to determine $\mathbf{k}_{sz}$ for each of the two scattered waves.

How this works out in practice is illustrated first in Figure 5 for the familiar case where the incident wave vector is in the x-z plane and the water wave vector is parallel to the x-axis. This is an example where the water roughness spectrum is 1-D, the scattering problem is 2-D (in x and z), and there is no out-of-plane scattering. The horizontal component of the incident wave vector is shown in the upper left in Figure 5 with the water wave crests shown with blue lines. In general there will be both a reflected wave and the two scattered waves. The reflected wave has the same horizontal component of the wave vector as the incident wave as shown in the upper right in Figure 5, while the horizontal components of the wave vectors for the two scattered waves will differ from the reflected component by $\pm \Delta \mathbf{k}$. The situation in the vertical plane is shown in the lower right in Figure 5. Since the wave vectors all have the same magnitude, they all lie on a common circle. For the scattered wave with an increased horizontal component (increased by $\Delta \mathbf{k}$), the vertical component must decrease to maintain the same vector magnitude, so the grazing angle of the scattered wave is decreased. For the scattered wave with a decreased horizontal component (decreased by $\Delta \mathbf{k}$), the vertical component must increase to maintain the same vector magnitude, so the grazing angle of the scattered wave is increased. While these results are familiar for the case of a 1-D surface spectrum (2-D scattering problem), the same considerations apply to the case of a 2-D surface spectrum (3-D scattering problem) where the results are not as familiar and indeed can be surprising.
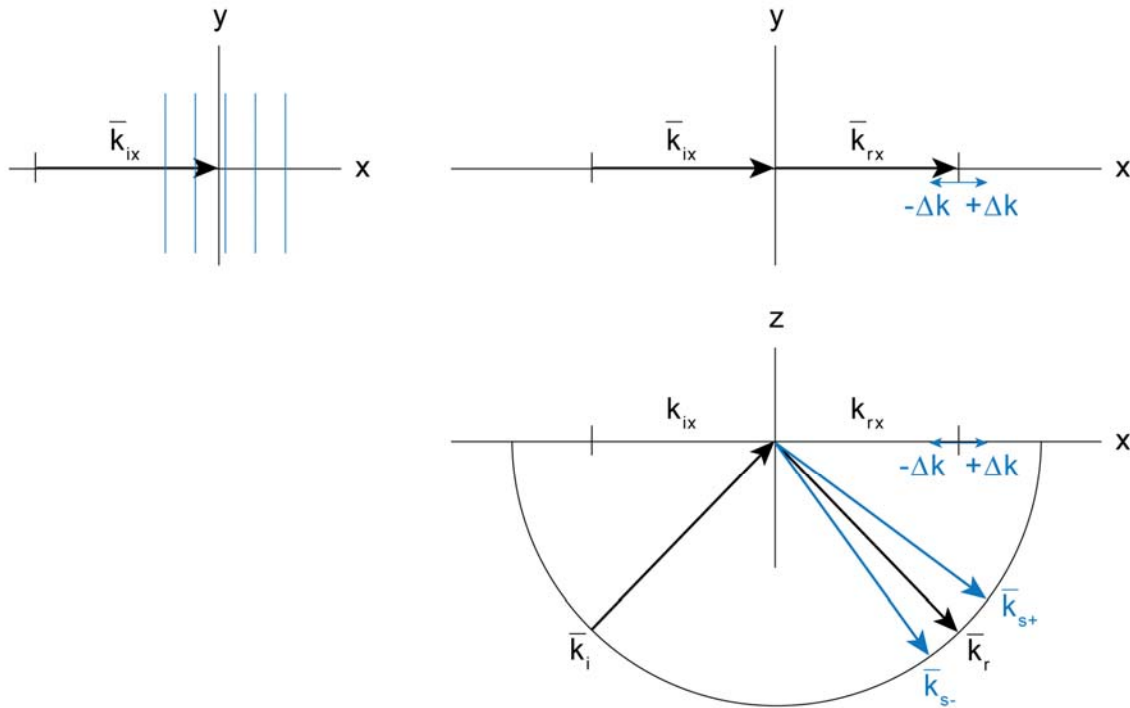

Figure 5. Wave vectors associated with scattering from a water wave traveling in the same direction as the horizontal component of the incident wave.

Figure 6 shows the wave vector diagrams for the more general case where the propagation direction of the water wave (shown in the upper left in Figure 6) is not parallel to the horizontal component of the incident acoustic plane wave, which is again taken to be parallel to the x-axis. The horizontal components of the two scattered acoustic waves (shown in the upper right in Figure 6) are again determined by vector addition of the horizontal component of the incident wave vector and the water wave vector, in this case leading to out-of-plane scattering. For the case shown, one scattered horizontal wave vector, denoted with a plus sign, will lead to a smaller z component than the incident wave, and thus to a smaller grazing angle in the scattered wave. The other scattered wave will have a higher grazing angle than the incident wave.

An interesting case occurs when the direction of water wave propagation is perpendicular to the horizontal component of the incident acoustic wave as illustrated on the left in the middle of Figure 6. The wave vector addition shown on the right in the middle of Figure 6 gives a symmetric result with the two scattered horizontal wave vectors having the same length that is longer than the horizontal component of the incident and reflected wave vectors. This means that both scattered waves will have a smaller grazing angle than the incident wave and will be symmetrically out-of-plane, one with a positive y-component, and the other with an equal but negative y-component. Viewed in the vertical x-z plane (shown in the lower right on Figure 6), the two scattered wave vectors will be co-incident and lie above the reflected x-z component and with the same x-component. The magnitude of the full scattered wave vectors will again be unchanged from the magnitude of the incident wave vector, but their projections on the x-z plane are smaller, since the y-component is not evident in this view.

This observation leads to important predictions about how the reverberation level will differ between the cases when the dominant waves are roughly parallel to the reverberation track compared to when they are approximately perpendicular to the reverberation track. In the first (parallel) case, surface scattering will lead to enhanced energy loss into the bottom reducing the expected reverberation, but the higher grazing angles incident on the bottom because of the surface scattering will mitigate that reduction to some extent. In the second (perpendicular) case, surface scattering will reduce the energy loss into the bottom, even compared to a calm surface, which should increase the energy that reaches longer ranges with a tendency to increase the longer range reverberation. But at the same time, the surface scattering will have the effect of decreasing the grazing angles at the bottom, which will mitigate the expected increase to some extent. How these contrary tendencies play out will be best understood with reverberation measurements and simulations.

The situation with modes is analogous. Scattering that increases the grazing angle causes coupling from a mode n to mode m, where m > n. Conversely, scattering the decreases the grazing angle causes coupling from a mode n to mode m, where m < n. So, in the ideal case where the water waves are all perpendicular to the reverberation track, surface scattering will only cause conversion to lower modes, producing a lower mode distribution than if the surface had been flat. This ideal case should lead to propagation to

longer ranges than if the surface was calm, and probably higher reverberation at longer ranges. Usually, however, the wave spectrum is spread over a range of azimuthal angles, and such an ideal case is not likely to occur.
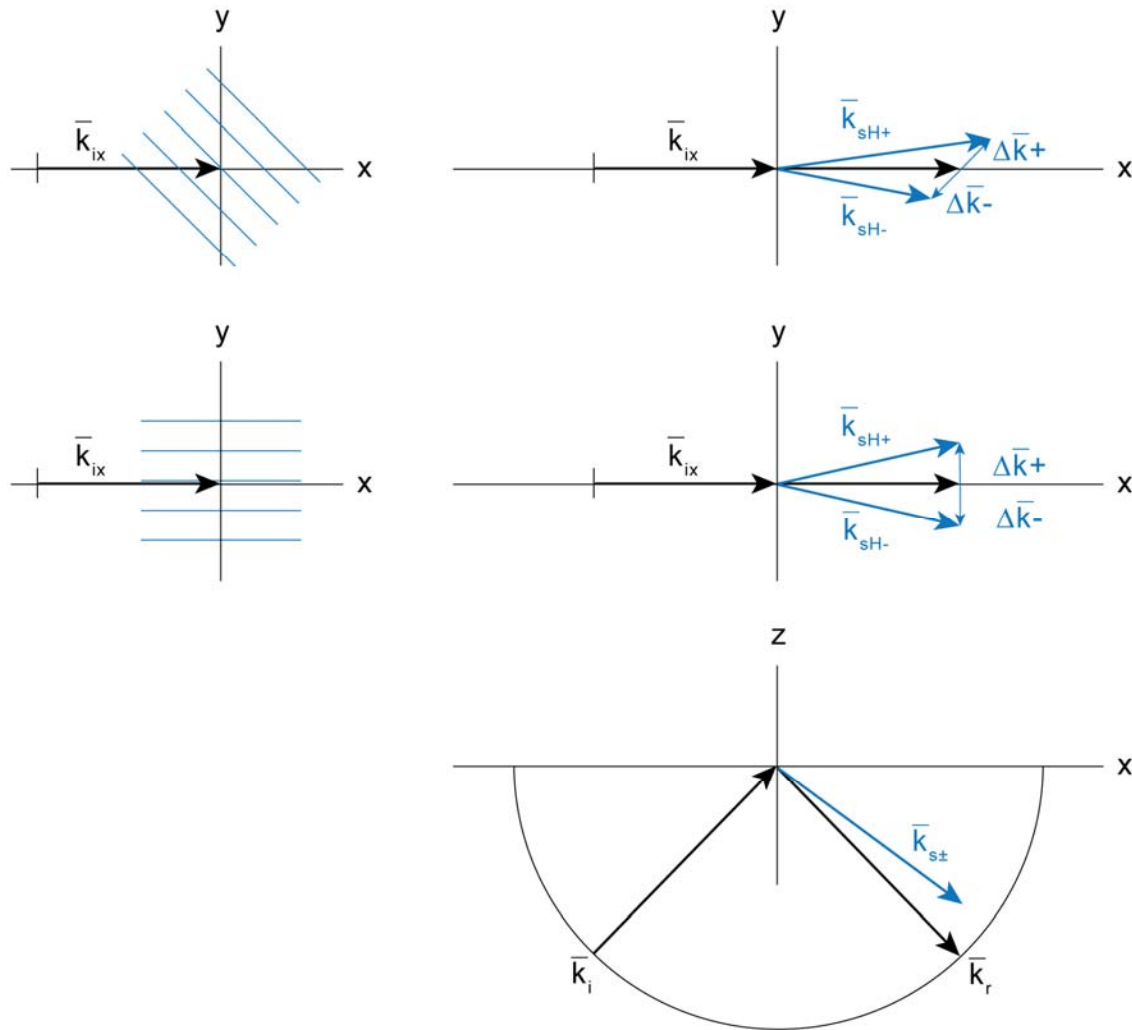

Figure 6. Wave vectors associated with scattering from a water wave traveling about 45°(top) and 90°(middle and bottom) from the direction of the horizontal component of the incident wave.

TREX13 provided several reverberation data sets that could be used for data/model comparisons. Figure 7 shows the reverberation level on three days when it was determined that there was no significant scattering from schools of fish. The two-way travel time has been converted to range using the average sound speed in the water. These curves are 10-ping averages, and the obvious spikes in the reverberation were found to be not statistical fluctuations, but deterministic returns from the regions with mud concentrations in the low points (the swales) in the gentle ridge and swale structure in the region of the experiment site. The spikes are likely the result of scattering from inclusions, such as clumps of sand or shell pieces, in the mud. This complicates making data/model

comparisons, since our modeling of the reverberation is confined to the sand on the ridges where there is information on the sediment roughness that can be used to model backscattering from the bottom. Ideally, then, the modeled reverberation curves should lie along the lowest portion of the data curves, not influenced by the spikes in the data.
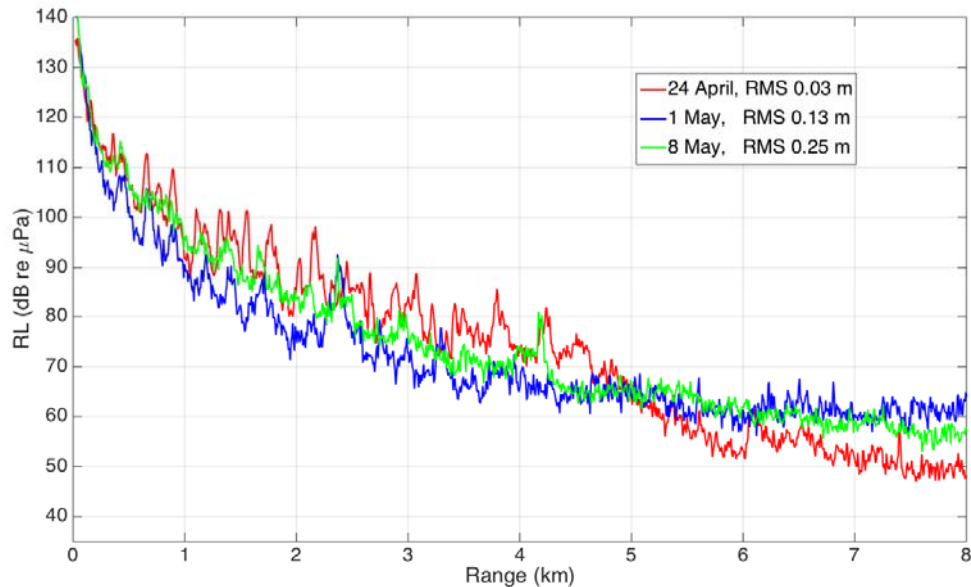

Figure 7. TREX13 measured reverberation level in the 3.4-3.5 kHz band on three days with different surface roughness.

It was also determined that the sediment changed character to become a softer sediment at a range greater than about 5 km, and in this region the reverberation level was also approaching the background noise level. Thus, the portion of the reverberation data out to a range of about 5 km is the best for making data/model comparisons.

For the three reverberation curves shown in Figure 7, the sea conditions varied from a quite small wave height on 24 April to somewhat higher sea states on 1 May and 8 May, all in 2013. Directional frequency spectra for the latter two days are shown in Figure 8, where the 2° wide reverberation track at a bearing centered on 129° is shown by the magenta line. These wave spectra show the direction the waves are traveling from, and it can be seen that on 1 May the waves are traveling from southeast to northwest relatively close to the reverberation track, and on 8 May they are closer to perpendicular to the reverberation track. In both cases there appears to substantial angular spread in the wave spectrum.

Simply from a comparison of Figures 7 and 8, some qualitative agreement with the discussion related to Figures 5 and 6 can be observed. With waves traveling approximately along the track, surface forward scattering should lead to a reduced

reverberation level for 1 May compared to the relatively calmer conditions for 24 April, and that is indeed the case in going from the red to the blue data curves in Figure 7. For 8 May the sea state was higher than for 1 May (the RMS height nearly twice as great), and if the wave direction were similar to that for 1 May, the reverberation level should be even lower than that for 1 May. But the wave direction is closer to perpendicular to the reverberation track, and according to the discussion related to Figure 6, that should lead to less reduction in reverberation level than if along the track, and in fact the reduction is even less than for the 1 May case. This shows qualitatively the importance of the directional nature of the wave field when modeling reverberation, and the need to account for such 3-D effects.
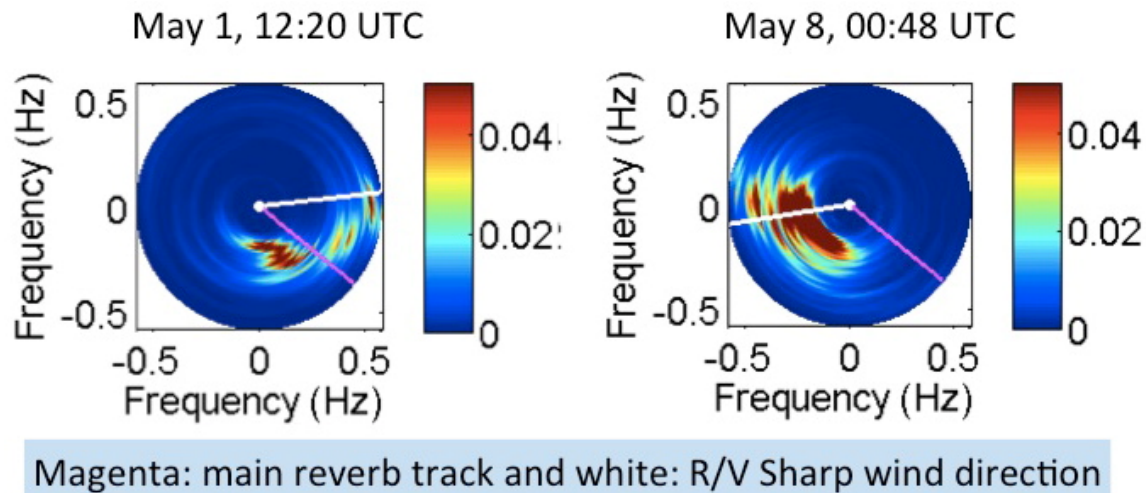

Figure 8. Directional frequency spectra for 1 May and 8 May 2013 at the TREX13 site from wave buoy data obtained by Peter Dahl and David Dall'Osto.

To proceed with modeling the reverberation, the 2-D frequency spectra as in Figure 8 where converted to 2-D wave number spectra, where the gravity wave dispersion relation was employed. Scattering from the bottom was modeled as scattering from only the rough water-sediment interface using roughness spectra obtained with a laser line scanner by Todd Hefner at APL-UW. The sound speed profile was very close to uniform with depth, and was taken as isovelocity. Finally, the known source level was used. With the scattering and propagation properties determined, there were no adjustable parameters when modeling the reverberation level.

It was first shown that adequate data-model comparisons were not obtained by starting with the 2-D wave number spectrum and then obtaining an equivalent 1-D roughness spectrum for use in transport theory by taking the marginal spectrum along the track, that is, integrating over the 2-D spectrum in the direction perpendicular to the direction of the reverberation track. In retrospect, this is not surprising, since the use of the marginal 1-D spectrum is not based on scattering physics.

To improve on the use of a marginal 1-D spectrum, a new approach was implemented based on the following hypothesis: For reverberation modeling, the 2-D propagation

model should be formulated such that surface forward scattering leads to the same amplitude distribution in vertical scattering angles as for the full 3-D case. That is, in going from 3-D to 2-D, the vertical scattering distribution should be preserved, since this is the most important element in determining the distribution of grazing angles on the bottom that will affect loss into the bottom and backscattering from the bottom. The out-of-plane horizontal component of the scattering (i.e., the y-component in Figure 6) is assumed to largely cancel out and is not treated. This hypothesis allows the full 3-D scattering problem to be reduced to a set of 2-D scattering problems along each radial for which the wave spectrum provides information. These radials are at 4° intervals, giving 90 radials. However, rough surface scattering theory generally assumes the wave spectra have been symmetrized, meaning that here the spectra are made symmetric with respect to the origin in the polar representation being used, and the same is true for the mode coupling formalism used with our transport theory. With this convention, it is necessary to only take into account 45 radials that span 180° in azimuth. To implement this approach, the 2-D wave spectrum is decomposed into 45 1-D spectra, one for each radial. Then a mode coupling matrix is found by adding the contributions from each radial to each matrix element. The resulting coupling matrix is used for the transport theory run. Because the source and receiver are at slightly different depths, transport theory runs are made from each location and are combined with the bottom bistatic scattering cross section when computing the reverberation level.

Figure 9 shows the data/model comparison for the measured reverberation in the 3.4-3.5 kHz band on 24 April, the day with a very low sea state with an RMS height of just 0.03 m. As would be expected for this case, there is very little difference between ignoring surface forward scattering (red) and accounting for surface forward scattering (blue). Even for this nearly calm sea, there is enough loss at short range in the coherent field to give a noticeably lower reverberation prediction when the coherent field is used, equivalent to using a coherent reflection loss at the surface. The agreement between the measured reverberation and the transport theory result with forward scattering (blue curve) is reasonably good, given that this is an absolute comparison with no adjustable parameters. As mentioned previously, an ideal model result should lie along the low end of the measured reverberation, since the data spikes due to scattering from inclusions in the mud regions are not being modeled. Even so, a "perfect result" for the modeled curve would likely be a dB or two higher than what is shown in Figure 9. But since there are many uncertainties that enter into such a calculation, such as the exact source level, receive sensitivity, bottom roughness spectrum at the time of the measurement, and so on, the level of agreement is reasonably good. There does appear to be a more significant discrepancy in the first 1 km of range, with the model curve being too low. This discrepancy is not presently understood, and may be related to the lack of including a sediment volume contribution to bottom scattering.

Figure 10 shows the data/model comparison for the measured reverberation in the 3.4-3.5 kHz band on 1 May, and the corresponding frequency spectrum is shown on the left hand side of Figure 8. For all of these cases the red curve gives the result with no forward scattering (i.e., taking the sea surface as flat) and is the same. Thus in comparison to Figure 9, the reduction in measured reverberation level is evident, as is the reduction in

the modeled reverberation level when forward scattering is included. It does follow from Figure 10 that ignoring forward scattering altogether leads to a reverberation level that is too high, and using the coherently propagated field leads to a reverberation level that is too low, even for this rather modest sea state with an RMS surface height of 0.13 m. The significant wave height is greater by about a factor of 4, or is about 0.52 m (1.7 ft), not very large. When surface forward scattering is included (blue curve in Figure 10), the data/model comparison is reasonably good. However, if Figure 9 is used to fix any offsets due to a systematic error, then the blue curve in Figure 10 should also just skim the lower extent of the data curve, but it comes in higher than that. Thus, the combined agreement in Figures 9 and 10 is not as good as the apparent agreement in Figure 10 alone.
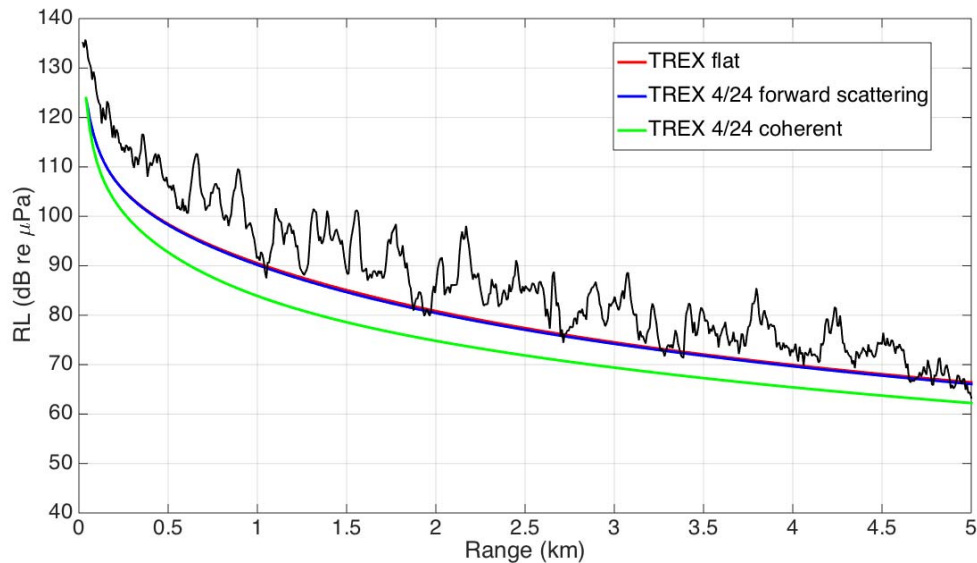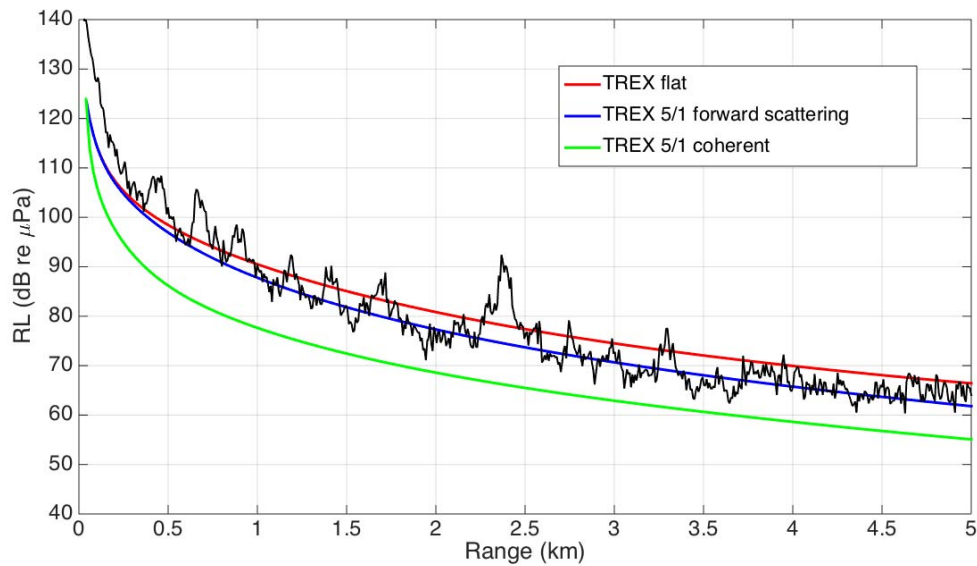

Figure 9. Data/model comparison for 24 April where the measured reverberation is shown with the black fluctuating curve. For the red curve, there is no forward scattering, for the blue curve, the 2-D spectrum is used to model the forward scattering, and for the green curve the coherent field is propagated, equivalent to the use of the coherent loss at the surface.

Figure 11 shows the data/model comparison for the measured reverberation in the 3.4-3.5 kHz band on 8 May, and the corresponding frequency spectrum is shown on the right hand side of Figure 8. Note that in this case the reverberation level is higher than the flat surface case out to a range of about 2.5 km, and then is about the same as the flat surface case at greater range. This is the type of behavior that might be expected if the wave field was narrowly confined in direction close to perpendicular to the direction of the reverberation track, as mentioned previously. However, the model curve with forward scattering (blue) differs significantly from the measured reverberation.

It can also be observed in Figure 11 that while the model result with forward scattering (blue curve) does not have a good match with the data, it does have a nearly uniform offset. Also, the coherent curve (green) lies much lower than the corresponding curve in Figure 10, consistent with the greater RMS surface height on 8 May.

The data/model discrepancy for 8 May seems to superficially lie with the wide angular extent of the frequency spectrum given on the right hand side of Figure 8, while the measured reverberation seems more consistent with a wave field that is confined more narrowly about a bearing perpendicular to the reverberation track. At least, that is how it appears based on the qualitative arguments discussed related to Figure 6. This led to considering the possibility that the angular spectrum given by the wave buoy might be inappropriately broadened. If so, that might explain the discrepancy.

Figure 10. Data/model comparison for 1 May where the measured reverberation is shown with the black fluctuating curve. For the red curve, there is no forward scattering, for the blue curve, the 2-D spectrum is used to model the forward scattering, and for the green curve the coherent field is propagated, equivalent to the use of the coherent loss at the surface.

To pursue this idea Todd Hefner helped obtain an independent set of frequency spectra measured with the Acoustic Wave and Current Profiler (AWAC) system during TREX13 and obtained by Joe Calantoni at NRL-SSC and Alex Sheremet at the University of Florida. This system is capable of measuring the direction frequency spectrum using a set of upward looking sonars. The directional frequency spectrum for the 8 May time period is shown in Figure 12. Initially, this directional frequency spectrum appeared promising, because the higher spectral levels appear more concentrated about a bearing closer to perpendicular to the reverberation track than in Figure 8 (right side). However, soon after Figure 12 became available, a more revealing version of the wave buoy spectrum for 8 May also became available and is given in Figure 13. In retrospect, the color scale chosen in Figure 8 did not fully represent the relative spectral levels and gave the impression that the spectrum had a broader angular range than it actually did.

While the spectra in Figures 12 and 13 are not in perfect agreement, the differences are modest. Figure 14 shows a comparison of the reverberation level with forward scattering using the wave buoy spectrum (blue) and the AWAC spectrum (yellow). The modeled

reverberation shows some difference between the two spectra, with slightly better data/mode agreement with the AWAC spectrum, but the difference does not remove the basic data/model discrepancy, which remains an open question. The difference shown can be viewed as one measure of modeling uncertainty as a result of environment uncertainty.
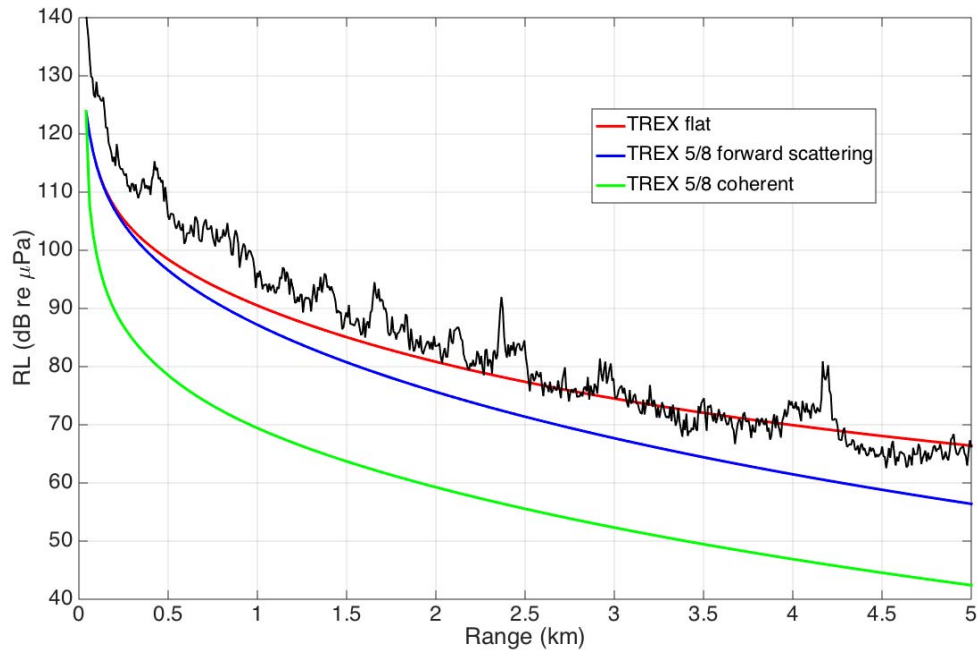

Figure 11. Data/model comparison for 8 May where the curves have the same meaning as in Figures 9 and 10.

Another possible contributor to the data/model difference for the reverberation on 8 May is suggested by a comparison of the reverberation data curves given by Figure 7. On 8 May the spikes in the data have reduced level in comparison to 24 April and 1 May. It may be that in the rougher conditions of 8 May the forward scattering leads to a smearing in time for the energy scattered from the mud regions, and this appears to increase the reverberation level in between the spikes that is being modeled as from only sand. This could be one reason the modeled curve is too low.

The results so far from TREX13 data/model comparisons can be summarized as follows: The importance of properly accounting for surface forward scattering and the directional nature of the wave field in reverberation modeling is evident in the measured reverberation itself. This shows the importance of taking into account the full 3-D nature of the forward scattering process when modeling the reverberation. The attempt to account for these effects by converting from 3-D to 2-D with an approximate method that preserves the vertical distribution of scattering angles shows some promise, but is not sufficiently accurate at this time. It should be noted that the TREX13 reverberation data were taken with relatively modest sea states, and at higher sea states these effects are predicted to be substantially greater.
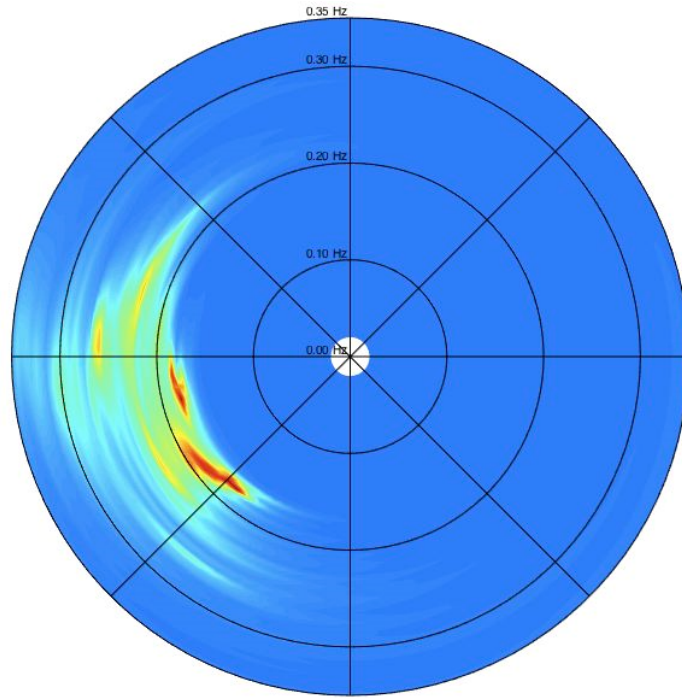
Figure 12. Directional frequency spectrum for 8 May obtained with the AWAC system by Joe Calantoni and Alex Sheremet. The colors are arbitrary and normalized to the maximum value.
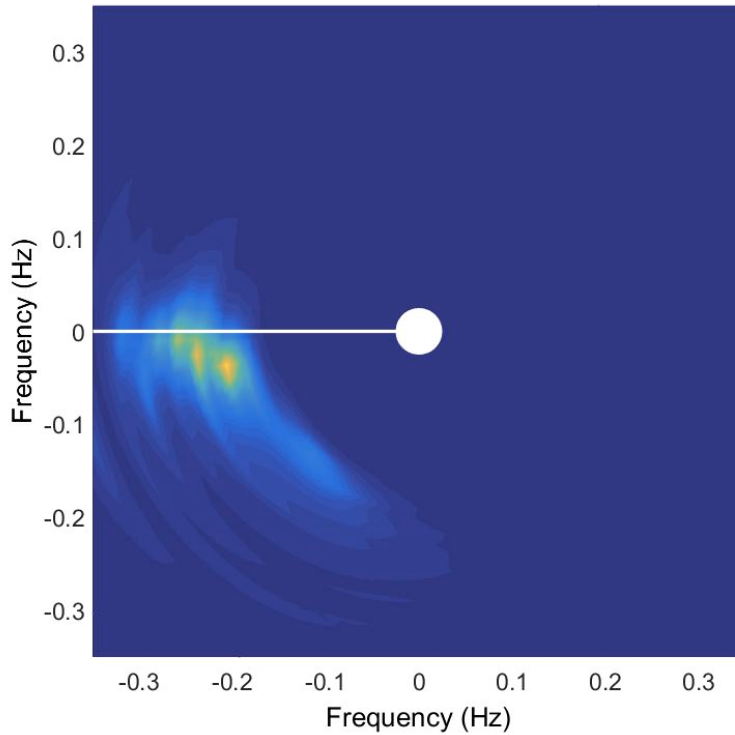

Figure 13. Frequency spectrum for 8 May from the wave buoy. The frequency range has been chosen to match the AWAC spectrum in Figure 12, and the colors indicate relative

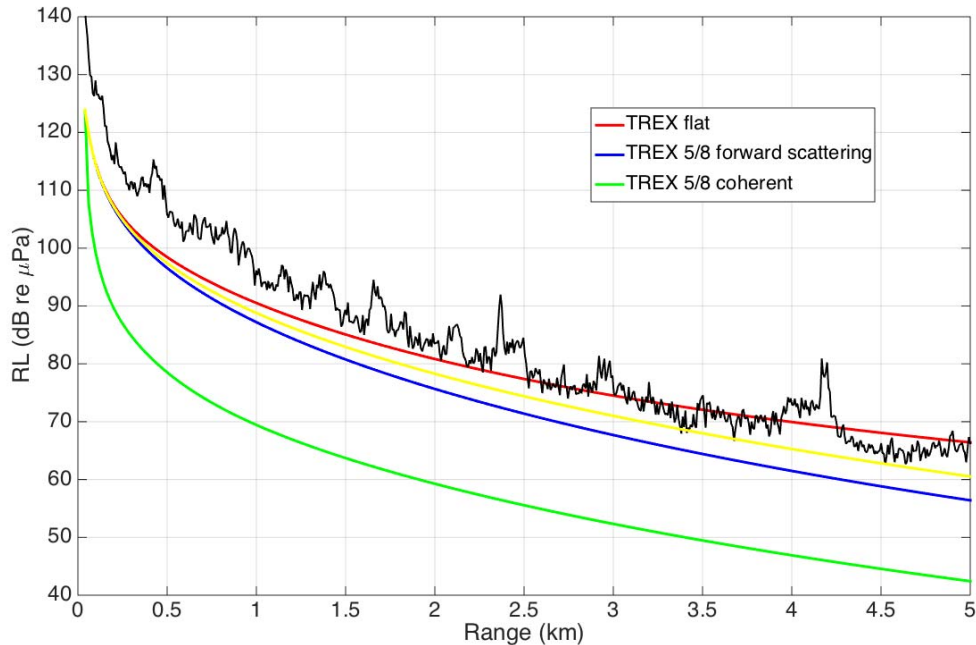*spectral level. The white line indicates a bearing due west.*

Figure 14. Data/model comparison for 8 May where the red, blue, and green curves were obtained with the wave buoy spectrum and where for the yellow curve the 2-D AWAC spectrum is used to model the forward scattering.

4. TOTLOS Model Development

Because transports theory has shown the importance of accounting for sea surface forward scattering in accurately modeling shallow water reverberation at mid frequencies, it becomes imperative to develop as approximate way to include these effects into traditional ray-based or mode-based reverberation codes. As mentioned in Section 1, a separate project initiated with support from PMW-120 (M. Speckhahn) has been ongoing with this particular goal in mind.

The approach being used in the development of TOTLOS will be summarized briefly. Because our transport theory is mode-based, it readily provides mode amplitudes as a function of range for any particular shallow water environment of interest. Each mode amplitude can be associated with a particular grazing angle at the sea surface. The decay of each mode amplitude over a cycle distance (the distance between surface interactions assuming reflected rays) is first determined, and the contribution of loss at the bottom is removed. What remains is identified as a loss in a single surface interaction, and in many cases that loss is negative, which means that there is a gain. In such a case more energy is being forward scattered into a particular mode than is being lost into the bottom in one cycle distance. With this information determined as a function of range for each mode, it is possible to form an effective reflection loss (the TOTLOS model) that will replicate the

transport theory results for propagation when surface forward scattering occurs. The model can then be tested in reverberation geometries using TOTLOS in a ray-based code such as CASS-GRAB and making comparisons with transport theory reverberation results.

The TOTLOS model depends not only on the sea surface roughness and frequency, but on range and on the water column and bottom properties, i.e., the TOTLOS model is scenario dependent. To avoid the need to tune the model to each scenario with appropriate transport runs, the approach is to develop an algorithm using quasi-analytic expressions for the model parameters based on a selection of transport runs, and then use that algorithm to define the parameters for the model in general

Continued progress has been made in developing the TOTLOS model for an effective reflection coefficient that leads to reverberation predictions in close agreement with transport theory results. At the present time, the TOTLOS model has been specialized to the case of an isovelocity sound speed profile with a 1-D roughness spectrum obtained by taking the marginal spectrum from an isotropic Pierson-Moskowitz roughness spectrum. Under these conditions the TOTLOS model can now handle variations in frequency, wind speed, water depth, sediment sound speed, sediment attenuation, and sediment density. We anticipate that when methods are perfected to treat the directional nature of the wave field with transport theory modeling of reverberation, then it should be possible to generalize the TOTLOS model to account for the same effects.

As part of an ongoing STTR Phase II supported by NAVAIR, TOTLOS is being implemented into ASPM. While the implementation of TOTLOS into CASS-GRAB was straightforward and effectively trivial, the case of ASPM is not as simple, and it has been an important component of the STTR project. As part of that effort, methods are being developed to obtain ground truth for reverberation in an environment with a range-dependent water depth based on a rough surface PE method for reverberation developed by Tang and Jackson. When that method is available, expected shortly, TOTLOS will be tested in range-dependent environments to determine the conditions under which the present version can be employed by using the local water depth in the model, while letting the depth vary with range.

A proposal has been submitted to ONR Code 322 to extend TOTLOS to account for general sound speed profiles (FY17) and to account for general 2-D surface roughness spectra (FY18). The latter effort would be based on the culmination of the work described previously to account for 2-D roughness spectra with transport theory.

REPORT DOCUMENTATION PAGE

1. REPORT DATE (DD-MM-YYYY)	**2. REPORT TYPE**	**3. DATES COVERED** (From - To)
20-07-2016	Final Technical	1/1/2013 - 3/31/2016

4. TITLE AND SUBTITLE
Transport Theory for Propagation and Reverberation

5a. CONTRACT NUMBER

5b. GRANT NUMBER
N00014-13-1-0216

5c. PROGRAM ELEMENT NUMBER

6. AUTHOR(S)
Eric I. Thorsos

5d. PROJECT NUMBER

5e. TASK NUMBER

5f. WORK UNIT NUMBER

7. PERFORMING ORGANIZATION NAME(S) AND ADDRESS(ES)
University of Washington - Applied Physics Laboratory
4333 Brooklyn Avenue NE
Seattle, WA 98105-6613

8. PERFORMING ORGANIZATION REPORT NUMBER

9. SPONSORING / MONITORING AGENCY NAME(S) AND ADDRESS(ES)
Office of Naval Research
875 North Randolph Street
Arlington, VA 22203-1995

10. SPONSOR/MONITOR'S ACRONYM(S)
ONR

11. SPONSOR/MONITOR'S REPORT NUMBER(S)

12. DISTRIBUTION / AVAILABILITY STATEMENT

Distribution Statement A: Approved for public release; distribution is unlimited.

13. SUPPLEMENTARY NOTES

14. ABSTRACT
There were two main goals proposed for this project. The first goal was test the accuracy of transport theory by making data-model comparisons with TREX13 reverberation results. The second goal was to use transport theory results to support the development of the TOTLOS model (an effective reflection loss for the total field) that will allow effects of sea surface forward scattering to be incorporated into standard ray-based, mode-based, or energy flux propagation and reverberation models. The stochastic process emphasized was forward scattering from the sea surface, which can affect predicted reverberation levels at mid frequencies by more than 10 dB. The results so far from TREX13 data/model comparisons show the importance of properly accounting for surface forward scattering and the directional nature of the wave field in reverberation modeling. The attempt to account for these effects by converting from 3-D to 2-D with an approximate method that preserves the vertical distribution of scattering angles shows promise, but is not sufficiently accurate at this time. It should be noted that the TREX13 reverberation data were taken with relatively modest sea states, and at higher sea states these effects are predicted to be substantially greater.

15. SUBJECT TERMS
Reverberation modeling, TREX13 data-model comparisons, and effects of sea surface forward scattering.

16. SECURITY CLASSIFICATION OF: U			**17. LIMITATION OF ABSTRACT**	**18. NUMBER OF PAGES**	**19a. NAME OF RESPONSIBLE PERSON** Eric I. Thorsos
a. REPORT U	**b. ABSTRACT** U	**c. THIS PAGE** U	UU	19	**19b. TELEPHONE NUMBER** *(include area code)* 206-543-1369